

10. Aerosol

S.No.	Product Name	Spatial Resolution	Temporal Resolution
1	3DIMG_L2G_AOD	0.10X0.10 degree	30 minutes

10. Aerosol Optical Depth (AOD) Reterival

10.1 Algorithm Configuration Information

10.1.1 Algorithm Name

Aerosol Optical Depth (AOD)

10.1.2 Algorithm Identifier

3DIMG_L2G_AOD

10.1.3 Algorithm Specification

Version	Date	Prepared by	Description
1.0	14.02.2007	Prakash Chauhan	AOD Baseline Document (Version-1)
1.1	17.08.2012	Prakash Chauhan Nivedita Sanwani Arvind Sahay	AOD Baseline Document (Version-2)
1.2	01.01.2021	Manoj K Mishra	AOD Baseline Document (Version-3)

10.2 Introduction

10.2.1 Overview and background

Aerosols play an important role in numerous aspects of human life. Aerosols have large-scale effects, such as their impact on climate by redistributing solar radiation (Herman and Browning 1975; Charlson *et al.* 1991; Haywood and Boucher 2000) and interacting with clouds (Platnick and Twomey 1994; Kaufman et al. 2002). Aerosol information is also critical for atmospheric correction algorithms for multi-spectral satellite sensors and military operations. The climate effects of atmospheric aerosols may be comparable to CO₂ greenhouse effects, but with opposite sign and larger uncertainty (Hansen and Lacis, 1990). Aerosols have a significant impact on human life beyond the climate element. When in the lower troposphere, aerosols cause poor air quality, reduction of visibility, and public health hazards. Satellite remote sensing provides a means to derive aerosol distribution at global and regional scales.

This Algorithm Theoretical Basis Document (ATBD) describes the updated algorithm used to retrieve the Aerosol Optical Thickness (AOD) for the INSAT-3D/3DR Imager instrument operating from a geostationary platform. In comparison to previous algorithm (see INSAT-3D AOD ATBD version-1&2), the present algorithm (version-3, Mishra et al, 2018) is significantly different both in terms of surface reflectance characterization as well as aerosol inversion. The updated algorithm has several advancement, which has improved the AOD product. Following points are some of the important features of the present algorithm that makes it advanced and improved in comparison to previous versions:

a) Previous algorithm utilizes single scattering approximation (SSA) that is it do not consider multiple scattering, while in present algorithm exact radiative transfer calculation are done considering multiple scattering events also.

- b) In previous versions, minimization of 30-day top of the atmosphere (TOA) radiance is assumed as surface contribution, while here minimization of Rayleigh corrected TOA reflectance is used for generating clear composite image (CCI).
- c) In previous version CCI image is directly used as surface reflectance, while in present algorithm CCI image is first atmospherically corrected using dynamic (seasonal and spatial) background aerosol database (generated using multiyear MODIS aqua AOD data) to generate surface reflectance which is then used for AOD inversion.
- d) Previously perfectly scattering aerosol type is assumed for both ocean and land (for land it is rarely valid), while in updated algorithm for AOD inversion continental and marine aerosols are used for land and ocean, respectively.
- e) In previous versions, AOD retrieval done for all pixel even over bright surface where in principle retrieval is not possible using band centered at red (650nm) wavelength, while in current version AOD retrieval is done only for those pixel where surface reflectance is less than critical reflectance. Thus, false retrievals such as AOD retrieval over very bright surface (like desert or bare arid soil surfaces or high reflecting urban setups) are reduced/masked.
- f) Current algorithm gives AOD product at 550 nm.

The output product description is summarized in Table 1. Specifically, this document identifies the sources of input data, both INSAT-3D/3DR imager and non- INSAT-3D/3DR imager data, required for retrieval; provides the physical theory and mathematical background underlying the use of this information in the retrievals; includes implementation details; and describes assumptions and limitations of the proposed approach.

Table 1: Summary of Aerosol Optical Depth (AOD) product

Parameter Name	Units	Horizontal Cell Size	Comments
Aerosol Optical depth at 550 nm	Dimensionless	10.0 km for both Land and oceans	Retrieved for all cloud free regions.

10.2.2 Objective

The objective of this algorithm is to calculate the aerosol optical thickness, proportional to the total aerosol loading of the ambient aerosol, over both land and ocean for Indian region on a six times (6:00, 6:30, 7:00, 7:30, 8:00 and 8:30 UTC) daily basis. Retrievals are only performed for cloud free pixels during the daytime. The overall objectives of the INSAT-3D/3DR aerosol retrievals algorithm is to determine the aerosol optical thickness, at 550 nm and 10 km spatial resolution over both land and ocean surfaces with root mean square (RMS) error of ± 0.20 . Optical thickness retrievals apply only under clear and daytime conditions.

10.3 Inputs

10.3.1 Static Data

Parameter	Resolution	Source
Digital elevation model (DEM)	5.0 minutes	ETOPO5
Relative Humidity climatology (monthly)	0.5 degree	NCEP
Spectral Response Function (SRF) for Imager bands	1nm	Sensor Group of Space Applications Centre, Ahmedabad

10.3.2 Image and preprocessing data (Dynamic)

Parameter	Resolution	Quantization	Accuracy	Source
Radiometric and geometric corrected radiance values of visible channel (0.55-0.75 μm)	4 km	10 bit	----	Derived from raw data by DP (data processing)
Radiometric and geometric corrected BT values of TIR-1 channel	4 km	10 bit	----	Derived from raw data by DP (data processing)
Radiometric and geometric corrected BT values of TIR-2 channel	4 km	10 bit	----	Derived from raw data by DP (data processing)
Geolocation file along with sun zenith & azimuth and sensor zenith and azimuth information	All pixels	---	Not greater than 1 pixel	Derived from raw data by DP (data processing)
At least 28-day previous data for Visible band should be available for 1130 and 0830 hrs. UTC for the generation of Clear composite reflectance image	4 km	---	---	Derived from raw data by DP (data processing)

10.3.3 Other Auxiliary data and Model Inputs

Parameter	Resolution	Quantization	Accuracy	Source
Total Column Ozone	50 km	--	--	NCEP

concentration				
Surface pressure	50 km	--	--	NCEP or GTS through IMD

10.4 Algorithm Functional Specifications

10.4.1 Overview

It has been demonstrated that aerosol optical thickness can be retrieved from solar-reflected radiance, and that aerosol size distribution information is carried in the spectral dependence of aerosol optical thickness (e.g., Kaufman et al., 1997; Kaufman et al., 2002). Thus, satellite reflectance measurement limited to one (GOES) or two channels (Advanced Very High Resolution Radiometer [AVHRR]) were used first to derive the total aerosol content by assuming a given aerosol model.

The relatively homogeneous surface of the ocean enables the direct application of the look up table (LUT) approach to find the aerosol optical thickness. Using the observed reflectance at the top of the atmosphere (TOA) in coordination with ancillary information on the wind speed, water vapor, surface pressure, surface elevation, and ozone, the corrected reflectances are inverted into a maritime LUT to find values of optical thickness.

The approach over land is more complicated, in that dark, vegetated surfaces are required for aerosol optical depth retrieval. In dark vegetation approach for aerosol retrieval a near-IR band is used to identify dark, vegetated pixels, then the surface reflectance in the visible bands is calculated from the observed reflectance in the near-IR band. The optical thickness is initially calculated assuming a continental aerosol model. The suspended matter information is used to choose a better aerosol model and more accurate values of optical thickness (Kaufmann et al. 1997).

In spite of advances in aerosol remote sensing over land, most retrievals are limited to once or twice per day, as by the morning and afternoon passes of the orbiting polar satellites. Aerosols, however, show diurnal variations that would be missed by such sparse observations. While studies of aerosol optical depth from Sun photometers show little systematic trends (Smirnov et al. 2002), surface observations of scattering show significant diurnal patterns (Bergin et al. 2001). It is required to understand aerosol plume movement to track and forecast plume movement in the interest of human health. Therefore, it is important to monitor the temporal aspects of aerosol.

The INSAT-3DR imager data from geostationary platform has the potential to provide aerosol observations over land and ocean with multiple observations per day. Many studies have demonstrated the potential of Geostationary Operational Environmental Satellite (GOES) series of imager sensors to provide quantitative estimates of aerosol optical (Knapp et al. 2002, Knapp et al. 2005). Their sensitivity studies, however, concluded that retrievals depend on aerosol optical property assumptions and surface reflectance. Studies using newer geostationary satellites (e.g. GOES-8) and larger validation networks (e.g. Aerosol Robotic Network—AERONET) supported those initial

findings. Specifically, Zhang et al. (2001) and Knapp et al. (2002) showed that aerosol monitoring from GOES is possible for South America. However, this region has optimal retrieval conditions: surface cover with little variability (i.e. rainforest) and large aerosol optical depths (from biomass burning).

Studies by Knapp et al. (2005) have shown operational potential of GOES series of sensors for the monitoring of aerosol optical depth over land. A method is proposed by Knapp et al (2005) to correct surface effects and retrieve aerosol optical depth using visible reflectance measurements from the Geostationary Operational Environmental Satellite (GOES). The surface contribution is determined from temporal compositing of visible imagery, where darker pixels correspond to less atmospheric attenuation and surface reflectance is deduced from the composite using radiative transfer. The method is applied to GOES-8 imagery over the eastern US. Retrieved surface reflectance is compared with separate retrievals using a priori ground based observations of aerosol optical depth.

10.4.1.1 Theoretical Background

The INSAT-3DR imager data will be used to perform the surface reflectance and aerosol optical depth retrievals and mask for clouds. It measures top of the atmosphere (TOA) radiance in six channels: three at infrared wavelengths, one in the visible wavelength and one sensitive to both solar and Earth-emitted radiance. Primarily, the visible channel (0.52–0.72 μm full width at half maximum) is sensitive to aerosol scattering and remaining channels are used for cloud masking. The cloud mask algorithm is based on the Clouds from the Advanced Very High Resolution Radiometer (AVHRR) (CLAVR) algorithm (Stowe et al. 1999) which uses spectral and spatial thresholds to test for the presence of clouds.

The retrieval of aerosol information from INSAT-3DR imager data is a 3-step process:

- 1) Cloud masking
- 2) Composite the visible images to estimate the surface reflectance, and
- 3) Use the surface reflectance with an image to retrieve the aerosol optical depth.

These steps are described below.

Cloud Masking of INSAT-3DR Imager data

Clouds are generally characterized by higher reflectance and lower temperature than the underlying earth surface. As such, simple visible and infrared window threshold approaches offer considerable skill in cloud detection. Following threshold-based tests will be performed to detect the cloudy pixels.

a) Visible band threshold test

The reflectance threshold test using visible band of INSTA-3D/3DR. Pixels with visible channel reflectance greater than 0.3 over land and greater than 0.10 over ocean are considered cloudy.

b) TIR Brightness temperature threshold test

Pixels with brightness temperature in TIR1 channel less than 273 are considered cloudy.

c) Standard deviation threshold test

Land: 3X3 pixel window is considered for calculating standard deviation in visible and TIR1 channel. If standard deviation of visible channel and TIR1 BT is greater than 0.03 and 4, respectively than all pixels in 3X3 window are masked.

Ocean: 3X3 pixel window is considered for calculating standard deviation in visible and TIR1 channel. If standard deviation of visible channel and TIR1 BT is greater than 0.015 and 1, respectively, than all pixels in 3X3 window are masked.

Surface Reflectance Retrieval

Estimating the surface contribution to the TOA INSAT-3D/3DR Imager visible reflectance is difficult since observations will have atmospheric contamination. For instance, a visible observation from INSAT-3DR Imager on a cloudless day with low aerosol burden will still have gaseous absorption (primarily, ozone and water vapour); Rayleigh scattering; and residual aerosol extinction. This atmospheric component to the TOA reflectance needs to be removed to retrieve the surface reflectance. While studies have shown it is possible to estimate the surface component from observations in the near infrared (e.g. 2.1 μm) where aerosol and Rayleigh scattering are very low (Kaufman et al. 2002), the INSAT-3D/3DR imager lacks an observation at this wavelength. Therefore, a compositing method will be used to estimate the surface reflectance.

The INSAT-3D/3DR visible channel radiance is converted to top of the atmosphere (TOA) reflectance. TOA reflectance is then corrected for ozone and water Vapor absorption. Water vapour and ozone concentration are used from NCEP model data. Further Rayleigh reflectance is removed from the gaseous absorption corrected TOA reflectance to get Rayleigh corrected reflectance. This reflectance has aerosol and surface contribution only. Now for each pixel, the 30 day previous Rayleigh corrected reflectance is sorted and first and second minima is computed. First minima represent the clearest condition, however, due to cloud shadow contamination, sometimes first minima may not be the true representative of surface reflectance, therefore to remove shadow effect, and we put a threshold test on first minima. If first minima are less than 0.04 then second minima will be considered otherwise first minima is considered. The threshold of 0.04 on first minimum to avoid shadow effect is empirical. This sorting of Rayleigh corrected reflectance and selection of first or second minima is done for all pixel to obtain clear composite image. By using this value to obtain the surface reflectance, one assumes that aerosol would increase the reflectance and cloud shadows will be rare. The length of the time is somewhat subjective. In general, a long enough time is needed for at least one cloud-free observation. Knapp et al. (2005) used a two week (i.e., 14 day) period. The clear composite reflectance is then corrected for background aerosol optical depth (0.02 and 0.04 for ocean and land respectively) to estimate Lambertian surface reflectance (ρ_{surf}). The image in figure (1) shows Lambertian surface reflectance computed using above mentioned method from INSAT-3D data from 4-31 December, 2013 and 4-31 January 2014 which is used for aerosol inversion on 1 January 2014 and 1 February 2014, respectively.

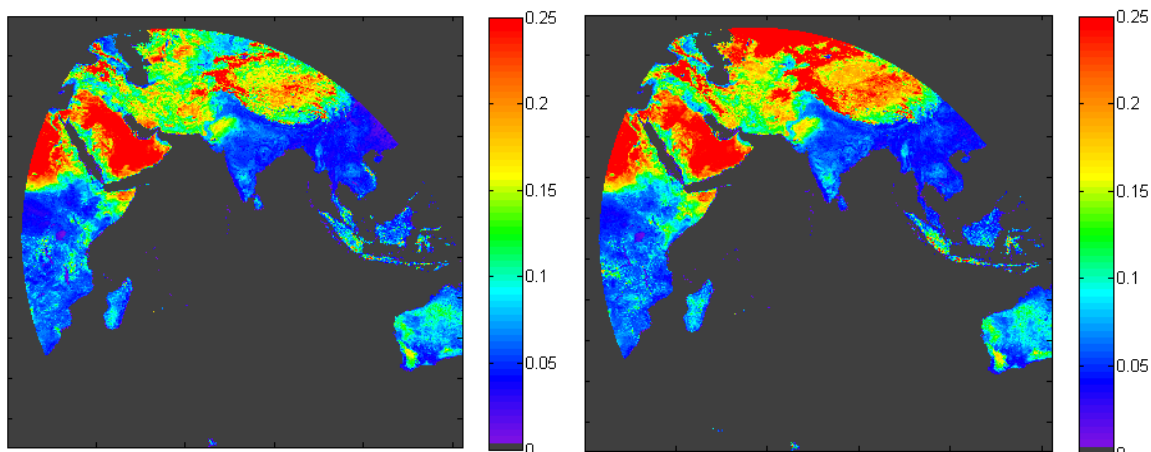


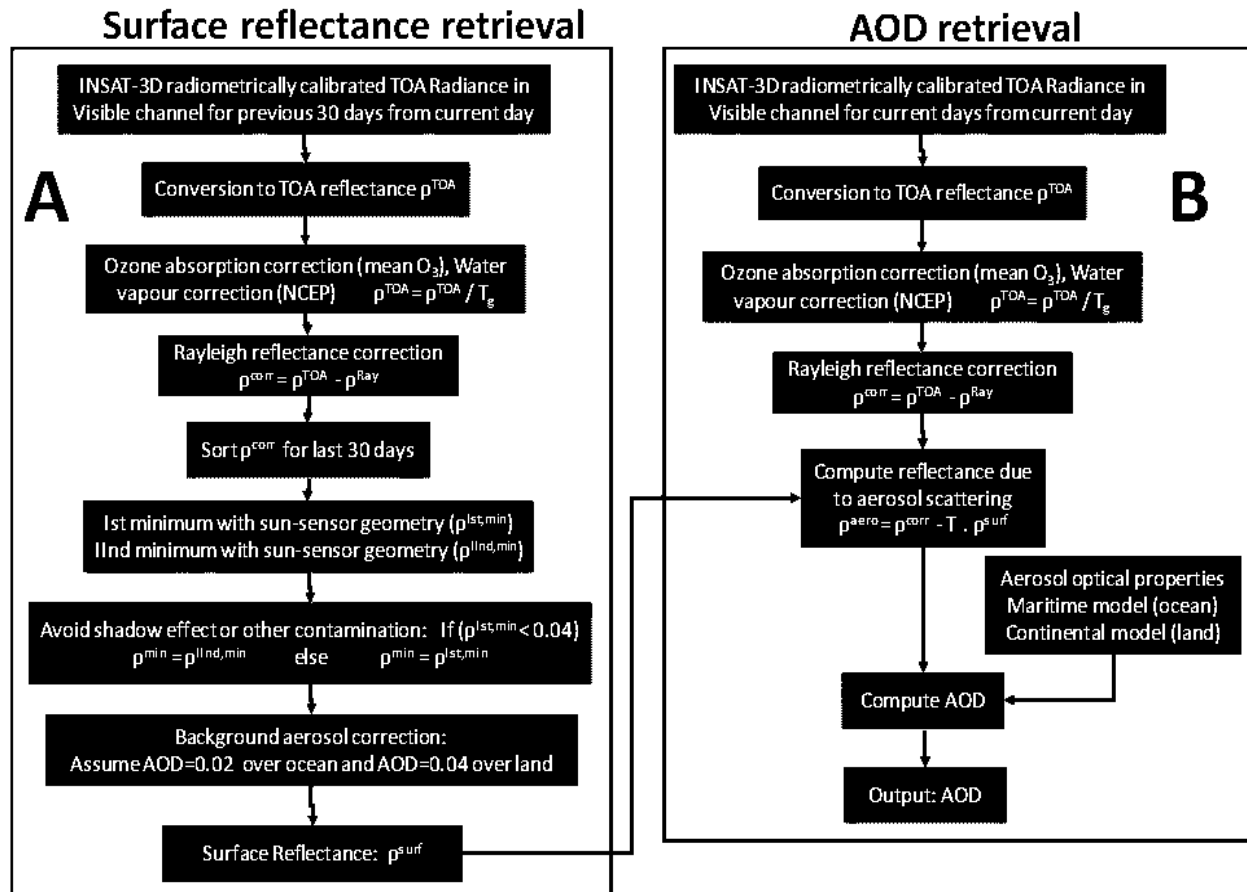
Figure 1. Shows Lambertian surface reflectance derived from clear composite method using INSAT-3D visible channel data (a) derived from data for the period of 4-31 December 2013. (b) Derived from data for the period of 4-31 January 2013.

The accuracy of the composite depends on the length of time used to create it. For instance, enough cloud-free observations must exist with little aerosol influence for the surface reflectance to be accurate. Areas of persistent aerosol or cloud cover will be likely to have caused errors in the retrieved surface reflectance because the atmospheric component remains large in such situations. It is to be noted that in previous version of AOD retrieval algorithm (version 1 and 2), instead of minimizing Rayleigh corrected reflectance, the TOA radiance was minimized, therefore the effect of change in solar zenith angle during the period of previous 30 days decreases the accuracy of derived surface reflectance.

Aerosol Optical Depth Retrieval

The aerosol optical depth retrieval is performed using an INSAT-3D/3DR imager visible image and the retrieved surface reflectance (from the previous step). In this retrieval, the current day TOA reflectance is corrected for ozone and water vapour absorption and also corrected for Rayleigh reflectance. Then precomputed look tables (using 6S radiative transfer model) that consist spherical albedo, reflectance, transmittance as a function of sun-sensor geometry and aerosol optical thickness are used to simulate theoretical Rayleigh corrected reflectance which is then compared with observed Rayleigh corrected INSAT-3DR reflectance to obtain aerosol optical depth. It is to be noted that over land continental aerosol model is used while over ocean maritime aerosol model is used. In previous versions of AOD retrieval algorithm, single scattering approximation was used for inverting AOD, assuming perfectly scattering aerosol (single scattering albedo assumed to be unity). Figure 2 shows the schematic flow chart of the aerosol optical thickness (AOD) retrieval procedure.

10.4.1.2 Flow Chart



10.4.2 Operational Implementation

Step 1: Conversion from gray count to visible radiance and TIR brightness temperature.

Step 2: Cloud Masking.

Step 3: Conversion of TOA radiance to TOA reflectance.

Step 4: Correction of TOA reflectance for gaseous absorption and Rayleigh scattering.

Step 5: Generation of clear composite image using darkest observation using last 28-days data.

Step 6: Atmospheric correction of clear composite image for background aerosol and generation of Lambertian surface reflectance.

Step 7: Correct current day visible data for gaseous absorption and molecular scattering.

Step 8: Invert current day Rayleigh corrected reflectance to get AOD using Lambertian surface reflectance and pre-computed LUTs.

10.5 Outputs

Parameter	Unit	Min	Max	Accuracy	Resolution
Aerosol optical depth at 550 nm	Dimensionless	0	5	15-20%	10 Km

10.5.1 format of the output and the domain

Lat , Lon, AOD ,

Domain :

40 to 40 N, 30 E to 120 E

10.6 Validation

10.6.1 Data required

Parameter	Resolution	Source
AERONET spectral AOD data	In-situ point observation	AERONET sites in India Kanpur, Gandhi college (Patna) and Jaipur
Spectral AOD using handheld sun-photometer	In-situ point observation	Data collection campaigns will be organized
MODIS AOD products	0.1 to 1 degree	Data available through internet

10.6.2 Methods of validation

AERONET data for Validation

Post-launch routine ground-based observations can be made using AERONET, and any of the several miscellaneous techniques, including the diffuse/direct method, aureole meters, and polarization measurements. AeRoNet (Aerosol Robotic Network) is a network of ground-based sun-photometers established and maintained by Brent Holben of Code 923 of the NASA Goddard Space Flight Center and Tom Eck of Raytheon ITSS. The sun-photometers measure the spectral aerosol optical thickness and sky radiance. In India 3 Aeronet sites namely Kanpur, Goa and Dharwar are providing systematic in-situ AOD measurements. Data from these sites will be used for validation of INSAT-3D/3DR derived AODs.

Post-Launch Special Field Experiments

Many of the present satellite observations are augmented by special field campaigns to provide ground-truth data for the satellite-derived measurements. The INSAT-3D/3DR Imager derived aerosol optical thickness measurements will be validated using hand-held sun-photometer. The details of these campaigns (timing, location, instrumentation, etc.) will be decided later on.

Post-Launch Satellite-Based Inter-comparisons

INSAT-3D/3DR Imager derived aerosol optical depths may be validated by comparing them with aerosol optical depths derived by other satellite sensors, such as MODIS. The basic inter-comparison technique involves three steps: 1) identification of locations where both sensors fly over at nearly the same time; 2) extraction of data for storage in an inter-comparison archive; 3) analysis of the differences between the measurements.

10.7 Technical issues (Limitation etc.)

Accuracy of the product depends on the accuracy of the radiation model to simulate the satellite radiances. However, the following limitations of the present study have to be kept in mind.

- (i) Characterization of surface reflectivity is critical of the study. Use of darkest observation for last 28 days provides mean reflectivity. This may also introduce significant errors in derived AOD, specially for the location with persistent AOD for long period.
- (ii) Due to single visible channel aerosol type is to be fixed which is in reality is not a good approximation. This may introduce large errors in retrieved AOD.
- (iii) Over bright surface and high aerosol loadings, TOA reflectance becomes insensitive to aerosol therefore; AOD over bright surfaces may have large uncertainty.

10.8 Future Scope

In future algorithms making use of INSAT-3D/3DR imager data for SWIR and MIR bands can also be attempted for characterization of surface reflectivity.

10.9 References

1. Bergin, M.H., Cass, G.R., Xu, J., Fang, C., Zeng, L.M., Yu, T., Salmon, L.G., Kiang, C.S., Tang, X.Y., Zhang, H. and Chameides, W.L., 2001, Aerosol radiative, physical, and chemical properties in Beijing during June 1999. *Journal of Geophysical Research*, 106, pp. 17 969–17 980.
2. Charston, R.J., Langer, J., Rodhe, H., Levoy, C.B. and Warren, S.G., 1991, Perturbation of the northern hemisphere radiative balance by backscattering from anthropogenic sulfate aerosols. *Tellus*, 43AB, pp. 152–163.
3. Hansen, J. E., and A. A. Lacis, 1990, Sun and dust versus greenhouse gases: An assessment of their relative roles in global climate change. *Nature*, 346, 713-719.
4. Haywood, J. and Boucher, O., 2000, Estimates of the direct and indirect radiative forcing due to tropospheric aerosols: a review. *Reviews of Geophysics*, 38, pp. 513–543.
5. Herman, B.M. and Browning, S.R., 1975, The effect of aerosols on the Earth-atmosphere albedo. *Journal of Atmospheric Science*, 32, pp. 1430–1445.
6. Kaufman, Y.J., Tanre, D., Remer, L.A., Vermote, E.F., Chu, A. and Holben, B.N., 1997, Operational remote sensing of tropospheric aerosol over land from EOS moderate resolution imaging spectroradiometer. *Journal of Geophysical Research*, 102, pp. 17051–17067.
7. Kaufman, Y.J., Tanre, D. and Boucher, O., 2002, A satellite view of aerosols in the climate system. *Nature*, 419, pp. 215–223.

8. Knapp, K.R., Vonder Harr, T.H. and Kaufman, Y.J., 2002, Aerosol optical depth retrieval from GOES-8: uncertainty study and retrieval validation over South America. *Journal of Geophysical Research*, 107, 10.1029/2001JD000505.
9. Knapp, K. R., Frouin, R, Kondragunta and Prados, A., 2005, Toward aerosol optical depth retrievals over land from GOES visible radiances: determining surface reflectance, *International Journal of Remote Sensing*.
10. Mishra, M. K., 2018, Retrieval of Aerosol optical depth from INSAT-3D Imager over Asian landmass and adjoining ocean: Retrieval uncertainty and validation, *Journal of Geophysical Research: Atmospheres* 123 (10), 5484-5508.
11. Platnick, S. and Twomey, S., 1994, Remote sensing the susceptibility of cloud albedo to changes in drop concentration. *Atmospheric Research*, 34, pp. 85–98.
12. Smirnov, A., Holben, B.N., Dubovik, O.V., O’Neill, N.T., Eck, T.F., Westphal, D.L., Goroch, A.K., Pietras, C. and Slutsker, I., 2002, Atmospheric aerosol optical properties in the Persian Gulf. *Journal of Atmospheric Science*, 59, pp. 620–634.
13. Stowe, L.L., Davis, P.A. and McClain, E.P., 1999, Scientific basis and initial evaluation of the CLAVR-1 global clear/cloud classification algorithm for the advanced very high resolution radiometer. *Journal of Atmospheric and Oceanic Technology*, 16, pp. 656–681.
14. Zhang, J., Christopher, S.A. and Holben, B., 2001, Intercomparison of aerosol optical thickness derived from GOES 8 imager and ground-based Sun photometers. *Journal of Geophysical Research*, 106, pp. 7387–7397.